

DEFORMATIONS OF HOLOGRAPHIC IMAGES

BY A. KALESTYŃSKI, B. SMOLIŃSKA

Institute of Physics, Technical University of Warsaw*

(Received February 28, 1970)

Deformations such as elongation and contraction of the holographic images are described in this paper. These are seen when inclining the hologram plane during recording or reconstruction, even in the case of the Fresnel and the Fourier processes. This effect has been described by using the Fresnel transform in corresponding coordinates.

1. Introduction

The deformation of holographic images connected with illumination of the holograms during their reconstruction and recording with light falling not normally to the hologram plane is of particular importance for the faithful reconstruction of the holograms in their back diffracted field. The holograms, when illuminated, produce diffracted beams in front of them as well as behind them, as shown in Fig. 1 [1,2]. These beams carry the same information concerning both amplitude and phase relations as the beams appearing behind the hologram. The images in the back diffracted field are considerably brighter than those in the transmitted field. The pictures observed in the back field appear as mirror images of pictures in the transmitted field with the hologram as the symmetry plane. After removal of the silver image from the emulsion the diffracting action of the hologram disappears completely. It is assumed that the "back diffraction" takes place at the silver crystals which form the photographic image.

The reconstruction of the hologram in the back diffracted field is most convenient when the hologram makes an angle φ with the illuminating beam, as shown in Fig. 1. In this case a certain distortion of the reconstructed image is observed, the same for both diffracted fields. These deformations can be eliminated if the photographic plate during recording of the hologram is placed so that it makes the same angle φ with the axis of the beam diffracted by the object. Reconstruction from these holograms with light falling also under an angle permits faithful images to be obtained. The observed distortions of the re-

* Address: Instytut Fizyki Politechniki Warszawskiej, Warszawa, Koszykowa 75, Polska.

constructed images are more clearly seen for two-dimensional objects. For this reason the investigation of this effect can be of importance for the Fourier process.

Furthermore, such distortion will be largely treated.

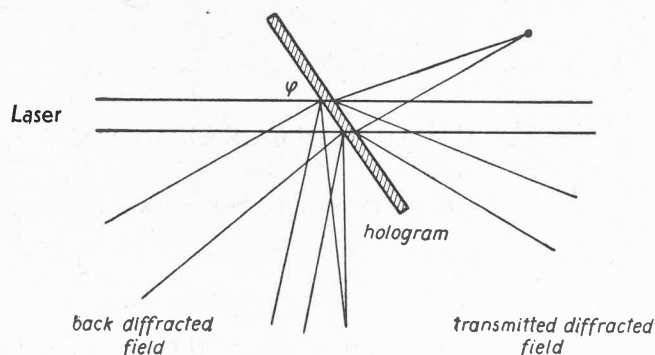


Fig. 1. Reconstruction of the hologram in the back and the transmitted field

2. Deformation of two-dimensional holographic images

2.1. Side band Fresnel holography formed with transmitted light

In order to describe the whole holographic process we introduce cartesian coordinates ξ, η for the object plane, x, y for the hologram plane and α, α for the image plane. The z axis corresponds to the direction of the plane wave illuminating either the object during recording, of the hologram during reconstruction.

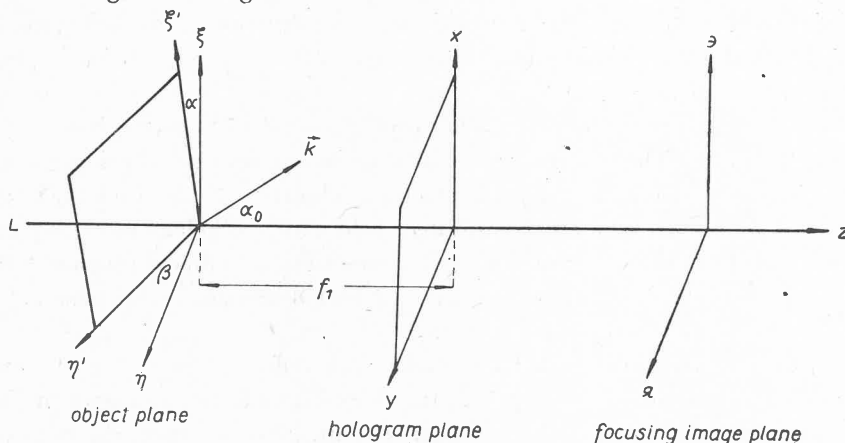


Fig. 2. Coordinate axes used in the description of the side band holography

For simplicity we restrict our description to a two-dimensional object (diapositive). This object lies in the plane defined by axes ξ', η' . The ξ' axis makes an angle α with the ξ axis, and the η' axis an angle β with η axis, as shown in Fig. 2. The light field illuminating the object is described by the complex amplitude $\psi_{01} = K' \exp\left(-\frac{i2\pi}{\lambda} z\right)$. The amplitude

transmittance of the object is $D(\xi', \eta')$. The direction of the reference wave makes an angle α_0 with the propagation direction z . In the hologram plane both beams interfere with each other, giving interference patterns. The intensity distribution $I(x, y)$ in the hologram plane is: $I(x, y) = |K \exp(i\mathbf{k}\mathbf{r}) + \psi_d(x, y)|^2$ where $K \exp(i\mathbf{k}\mathbf{r})$ is the reference field, $\psi_d(x, y)$ the field diffracted by the object, $\mathbf{k}\mathbf{r} = \frac{2\pi}{\lambda}(x \sin \alpha_0 + 2 \cos \alpha_0 z)$, $\mathbf{k} = \mathbf{i}k_x + \mathbf{j}k_y + \mathbf{k}k_z$, and $\mathbf{r} = \mathbf{i}x + \mathbf{j}y + \mathbf{k}z$.

We can say that the hologram sees the illuminated object in perspective shortening such that $\xi' = \xi \cos \alpha$ and $\eta' = \eta \cos \beta$. Then the object transmittance may given by $D(\xi, \eta) = D\left(\frac{\xi'}{\cos \alpha}, \frac{\eta'}{\cos \beta}\right)$. The transmitted and object-diffracted light field ψ_d can be described after Wellis [3] by paraxial approximation. Then,

$$\begin{aligned} \psi_d &= \iint \psi_{01} D\left(\frac{\xi'}{\cos \alpha}, \frac{\eta'}{\cos \beta}\right) \frac{\partial G\left(\frac{\xi'}{\cos \alpha}, \frac{\eta'}{\cos \beta}, x, y\right)}{\partial n} \frac{d\xi' d\eta'}{\cos \alpha \cos \beta} \\ &\cong K' \iint \psi_{01} D\left(\frac{\xi'}{\cos \alpha}, \frac{\eta'}{\cos \beta}\right) \exp\left\{\frac{i2\pi}{\lambda} R\left(\frac{\xi'}{\cos \alpha}, \frac{\eta'}{\cos \beta}, x, y\right)\right\} \frac{d\xi' d\eta'}{\cos \alpha \cos \beta} \quad (1) \end{aligned}$$

where G is the Green function of the Helmholtz equation, and

$$R = f_1 \left(1 + \frac{\left(\frac{\xi'}{\cos \alpha}\right)^2 + \left(\frac{\eta'}{\cos \beta}\right)^2}{2f_1^2} + \frac{x^2 + y^2}{2f_1^2} - \frac{\xi'x}{\cos \alpha} + \frac{\eta'y}{\cos \beta} + \dots \right).$$

The intensity distribution of the interference field recorded by a quadrate detector in the hologram plane is $I(x, y)$. Ignoring terms of higher order we may write the resulting transmittance of the hologram as

$$\begin{aligned} T(y, x) &= |I(x, y)|^{-\frac{\gamma}{2}} \\ &= |K|^2 - \frac{\gamma}{2} K'K^*C \exp\left(\frac{i2\pi f_1}{\lambda}\right) \exp\left\{\frac{i\pi(x^2 + y^2)}{\lambda f_1}\right\} \mathcal{D}(x, y) \exp(-i\mathbf{k}\mathbf{r}) \\ &= \frac{\gamma}{2} K'K^*C^* \exp\left(\frac{i2\pi f_1}{\lambda}\right) \exp\left\{\frac{i\pi(x^2 + y^2)}{\lambda f_1}\right\} \mathcal{D}^*(x, y) \exp(-i\mathbf{k}\mathbf{r}). \quad (2) \end{aligned}$$

Here,

$$\begin{aligned} \mathcal{D}(x, y) &= \iint D\left(\frac{\xi'}{\cos \alpha}, \frac{\eta'}{\cos \beta}\right) \exp\frac{i2\pi}{\lambda} \times \\ &\times \left\{ \frac{\left(\frac{\xi'}{\cos \alpha}\right)^2 + \left(\frac{\eta'}{\cos \beta}\right)^2}{2f_1} - \frac{\xi'x}{\cos \alpha} + \frac{\eta'y}{\cos \beta} \right\} \frac{d\xi' d\eta'}{\cos \alpha \cos \beta}. \end{aligned}$$

In this manner the information about the object which is seen in perspective shortening is recorded by the hologram.

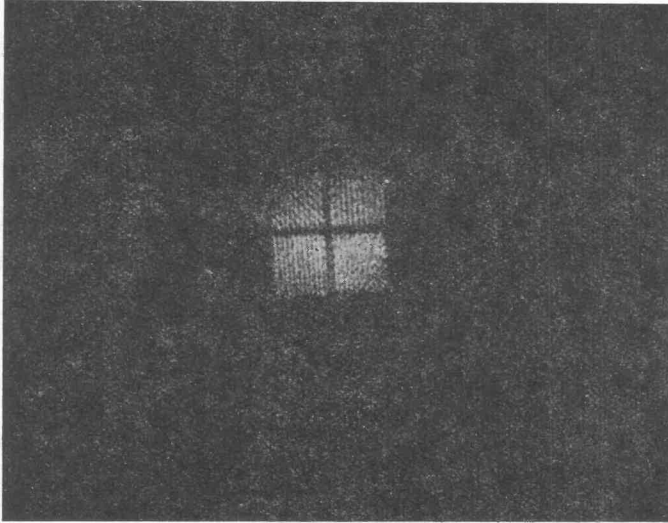


Fig. 3

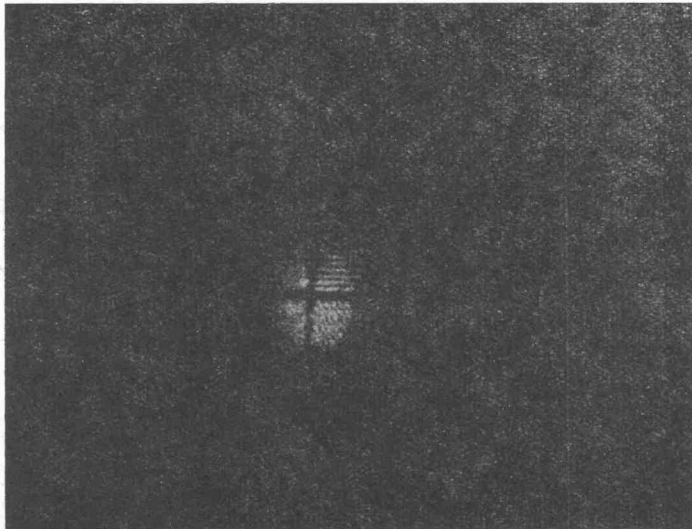


Fig. 3a

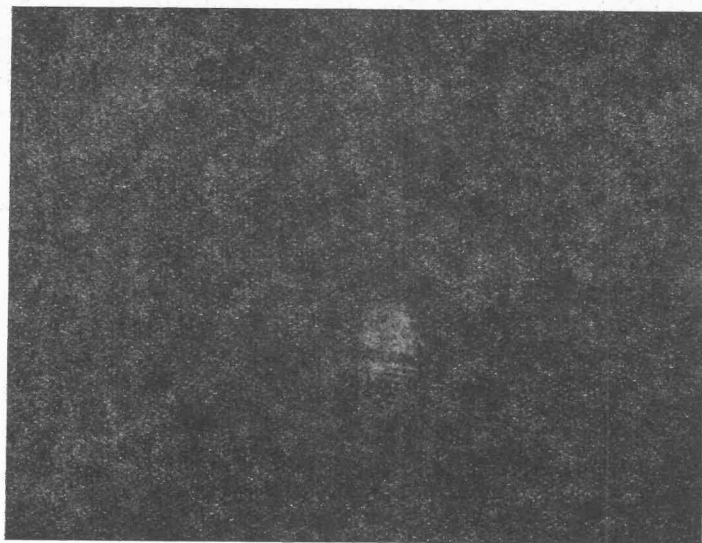


Fig. 3b

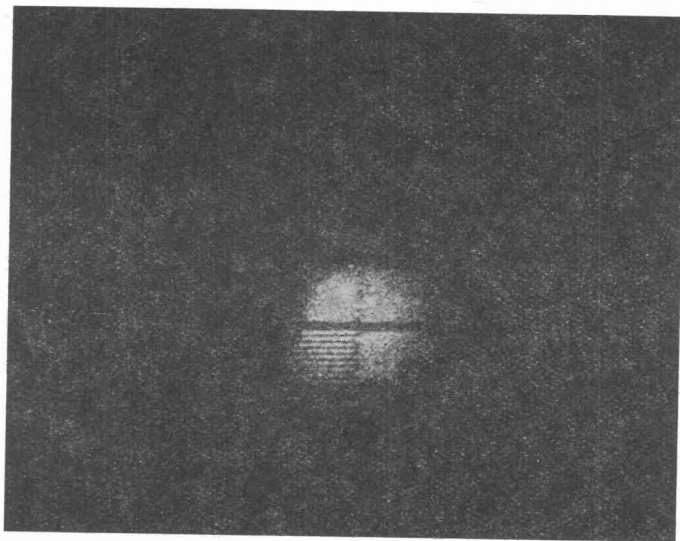


Fig. 3c

Fig. 3. Test image reconstructed from the side band hologram (ORWO WP3). *a.* The same test image reconstructed from the side band hologram when the object plane is rotated through an angle of 45° during recording. *b.* The same test image reconstructed from the side band hologram when the object plane is rotated through an angle 60° during recording. *c.* Reconstruction of the deformed test image shown in Fig. 3 when the hologram plane is rotated through an angle of 45° during reconstruction

During reconstruction of such a hologram, when a plane wave falls perpendicularly on the hologram, there appear three beams: the zero and the two diffracted beams, according to equation (2). The amplitude distribution $\psi_{\text{im}}(\vartheta, \varkappa)$ of either of the diffracted waves converging in the real image plane ϑ, \varkappa is given by

$$\psi_{\text{im}}(\vartheta, \varkappa) = \iint \psi_{02} T(x, y) \exp \left\{ \frac{i2\pi}{\lambda} \varrho(x, y, \vartheta, \varkappa) \right\} dx dy.$$

Substituting for $T(x, y)$ from equation (2) we have

$$\begin{aligned} \psi_{\text{im}}(\vartheta, \varkappa) = & -\frac{\gamma}{2} K' K C' C^* \exp \left(-\frac{2\pi f_1}{\lambda} \right) \cdot \int_{f_1=0} \int \exp \left(-\frac{i\pi(|x|^2 + |y|^2)}{\lambda f_2} \right) \times \\ & \times \mathcal{D}(x, y) \exp(i\mathbf{k}\mathbf{r}) \exp \left(\frac{i2\pi f_2}{\lambda} \right) \exp \left\{ \frac{i\pi}{\lambda f_2} \varrho(x - \vartheta, y - \varkappa) \right\} dx dy. \end{aligned} \quad (3)$$

Since ϱ is given by

$$\varrho \cong f_2 \left(1 + \frac{x^2 + y^2}{2f_2^2} + \frac{\vartheta^2 + \varkappa^2}{2f_2^2} - \frac{x\vartheta + y\varkappa}{f_2^2} + \dots \right)$$

equation (3) becomes

$$\begin{aligned} \psi_{\text{im}}(\vartheta, \varkappa) = A(\vartheta, \varkappa) \iint \tilde{F} \left(\frac{x}{\lambda f_1 \cos \alpha}, \frac{y}{\lambda f_1 \cos \beta} \right) \exp \left\{ 2\pi i \left[x \left(\frac{\sin \alpha_0}{\lambda} - \frac{\vartheta}{\lambda f_2} \right) - \right. \right. \\ \left. \left. - y \frac{\varkappa}{\lambda f_2} \right] \right\} dx dy \end{aligned} \quad (4)$$

where

$$A(\vartheta, \varkappa) = -\frac{\gamma}{2} K' K C' C^* \exp \left(-\frac{2\pi f_1}{\lambda} \right) \exp \left(\frac{i2\pi f_2}{\lambda} \right) \exp \left[\frac{i\pi}{\lambda f_2} (\vartheta^2 + \varkappa^2) \right] \exp \left(\frac{i2\pi f_1}{\lambda} \cos \alpha_0 \right)$$

and

$$\begin{aligned} \tilde{F} \left(\frac{x}{\lambda f_1 \cos \alpha}, \frac{y}{\lambda f_1 \cos \beta} \right) = \iint D^* \left(\frac{\xi'}{\cos \alpha}, \frac{\eta'}{\cos \beta} \right) \exp \left[-\frac{\left(\frac{\xi'}{\cos \alpha} \right)^2 + \left(\frac{\eta'}{\cos \beta} \right)^2}{\lambda f_1} i\pi \right] \times \\ \times \exp \left[\frac{i2\pi}{\lambda f_1} \left(\frac{\xi' x}{\cos \alpha} + \frac{\eta' y}{\cos \beta} \right) \right] \frac{d\xi' d\eta'}{\cos \alpha \cos \beta}. \end{aligned}$$

The integral in equation (4) represents the Fourier transform from coordinates x, y to coordinates $\sin \alpha_0 \cos \alpha f_1 - \frac{\vartheta \cos \alpha f_1}{f_2}, \frac{\varkappa \cos \beta f_1}{f_2}$. If the angle α_0 between the direction of the reference wave and z axis is small, then $\sin \alpha_0 \cong \alpha_0$. This corresponds to the case of a hologram with small resolution limit. In our case there were no more than 200 lines/mm on ORWO WP3 plates and 500 lines/mm on ORWO LP1 plates. The angle α_0 did not exceed

10°. In accordance with experiment we can take $f_1 = f_2$. Finally, from equation (4) we obtain:

$$\psi_{\text{im}}(\vartheta, \varpi) = AD^*(\vartheta \cos \alpha - f_1 \alpha_0 \cos \alpha, \varpi \cos \beta) \exp \left[-\frac{i\pi}{\lambda f_1} \{(\vartheta \cos \alpha - f_1 \alpha_0 \cos \alpha)^2 + \varpi^2 \cos^2 \beta\} \right]. \quad (5)$$

The observed intensity distribution is:

$$I_{\text{im}}(\vartheta, \varpi) = \psi_{\text{im}}^{\dagger}(\vartheta, \varpi) \psi_{\text{im}}^*(\vartheta, \varpi) = |A|^2 |D|^2 (\vartheta \cos \alpha - f_1 \alpha_0 \cos \alpha, \varpi \cos \beta).$$

This relation describes a reconstructed image which is shortened along the ϑ and ϖ axes and lies nearer to the zero beam. This effect is shown in Fig. 3. There are seen here pictures reconstructed from a hologram recorded in the above manner. From the photographs in Fig. 3a, b one can see the characteristic contraction described by equation (5).

Moreover, observations show that when the hologram is rotated during reconstruction, so that it makes an angle with the direction of the reconstructing wave, the observed defor-

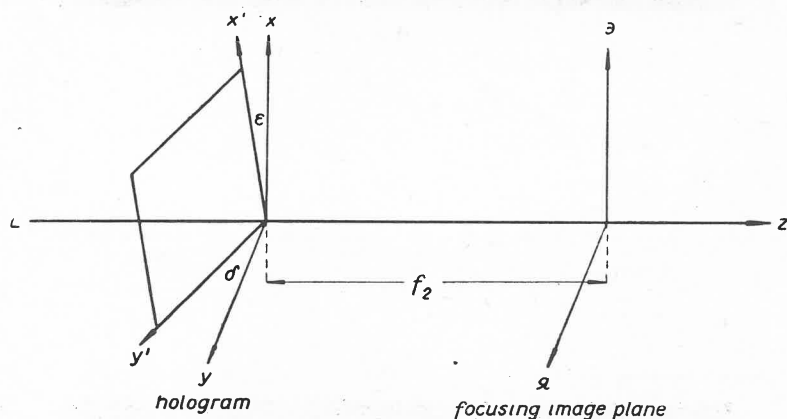


Fig. 4. Coordinate axes used in the description of reconstruction of side band hologram

mation is changed accordingly with the value of this angle. In such case the reconstructing wave "seen" the hologram in the $x'y'$ plane. It is lengthened according to the relations $x' = \frac{x}{\cos \epsilon}$ and $y' = \frac{y}{\cos \delta}$. This is because the x' axis makes an angle ϵ with the x axis and y' axis makes an angle δ with the y axis, as shown in Fig. 4.

The transmittance of this hologram can be now described in new coordinates by $T(x'y') = T\left(\frac{x}{\cos \epsilon}, \frac{y}{\cos \delta}\right)$. Consequently, the amplitude distribution of the wave diffracted by the hologram which focuses in the ϑ, ϖ plane is:

$$\psi_{\text{im}}(\vartheta, \varpi) = A(\vartheta, \varpi) \int F\left(\frac{-x}{\cos \alpha \lambda f_1}, \frac{-y}{\cos \beta \lambda f_1}\right) \exp\left(\frac{2\pi i}{\cos \epsilon} \left(\frac{\sin \alpha_0}{\lambda} - \frac{\vartheta}{\lambda f_2}\right) - \frac{y\varpi}{\cos \delta \lambda f_2}\right) \frac{dx dy}{\cos \epsilon \cos \delta}. \quad (6)$$

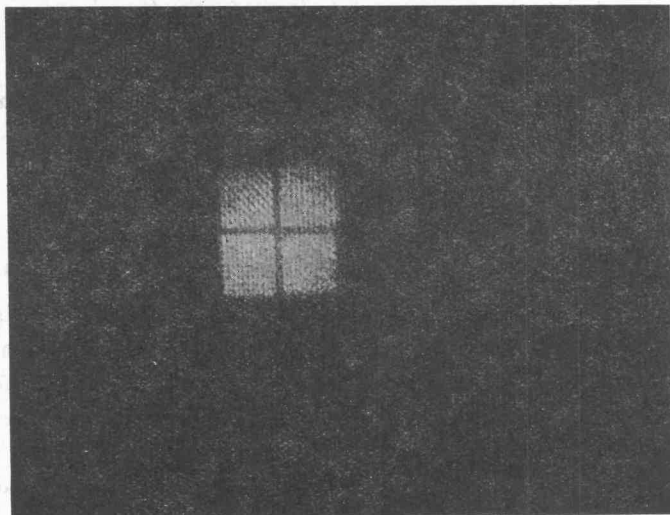


Fig. 5

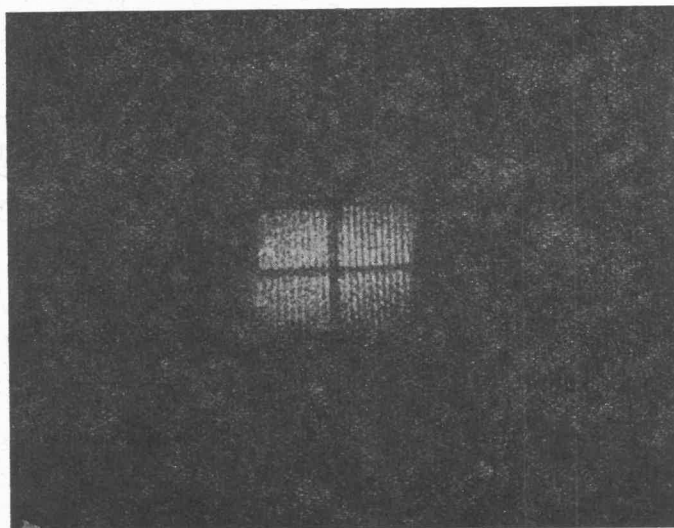


Fig. 5a



Fig. 5

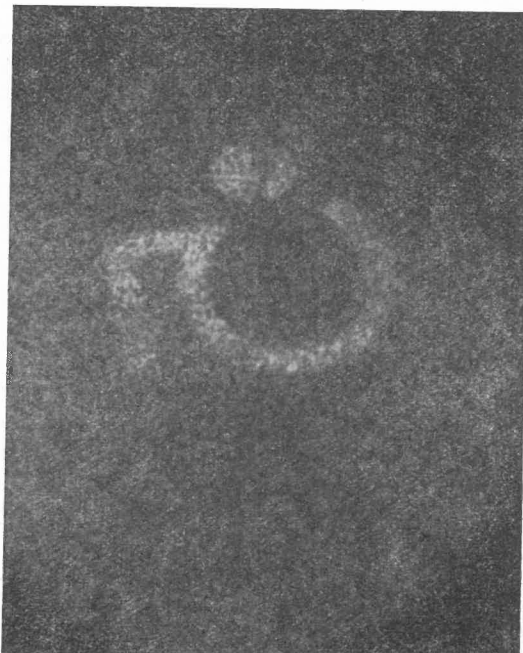


Fig. 5a

Fig. 5. Two different test images reconstructed from the side band holograms (ORWO WP3 Plattes). *a.* The same reconstructed test images when the hologram plane is rotated through an angle of 45° during reconstruction

This equation applies to the hologram which contains information about the perspectively deformed object. The integrand in equation (6) is

$$\begin{aligned} & \tilde{F} \left(\frac{-x}{\cos \alpha \lambda f_1} + \frac{-y}{\cos \beta \lambda f_1} \right) \\ = & \iint D^* \left(\frac{\xi'}{\cos \alpha}, \frac{\eta'}{\cos \beta} \right) \exp \left(-i\pi \frac{\left(\frac{\xi'}{\cos \alpha} \right)^2 + \left(\frac{\eta'}{\cos \beta} \right)^2}{\lambda f_1} \right) \exp \frac{i2\pi}{\lambda f_1} \left(\frac{\xi'_x}{\cos \alpha} - \right. \\ & \left. - \frac{\eta'_y}{\cos \beta} \right) \frac{d\xi' d\eta'}{\cos \alpha \cos \beta}. \end{aligned}$$

On taking the Fourier transform and assuming $f_1 = f_2 = f$, we obtain

$$\begin{aligned} \psi_{\text{im}}(\varrho, \varkappa) = & A(\varrho, \varkappa) D^* \left(\frac{\varrho \cos \alpha}{\cos \varepsilon} - f\alpha_0 \frac{\cos \alpha}{\cos \varepsilon}, \frac{\varkappa \cos \beta}{\cos \delta} \right) \times \\ & \times \exp \left[-\frac{i\pi}{\lambda f} \left\{ \left(\frac{\varrho \cos \alpha}{\cos \varepsilon} - f\alpha_0 \frac{\cos \alpha}{\cos \varepsilon} \right)^2 + \left(\frac{\varkappa \cos \beta}{\cos \delta} \right)^2 \right\} \right]. \end{aligned} \quad (7)$$

The observed intensity distribution in the ϱ, \varkappa plane is

$$I_{\text{im}}(\varrho, \varkappa) = |A|^2 \cdot \left| D^2 \left(\frac{\varrho \cos \alpha}{\cos \varepsilon} - f\alpha_0 \frac{\cos \alpha}{\cos \varepsilon}, \varkappa \frac{\cos \beta}{\cos \delta} \right) \right|.$$

Finally, the deformation of the reconstructed images depends both on how the hologram "sees" the object (this is determined by angles α and β) and how the reconstructing wave illuminates the hologram (this is determined by angles ε and δ). In the case when $\alpha = 0$, $\beta = 0$ and $\varepsilon \neq 0$, $\delta \neq 0$ the observed image is elongated in the direction of the ϱ and \varkappa axes, and the angle between the diffracted and the zero beam is enlarged in accordance

$$\text{with } \frac{1}{\cos \varepsilon}, \frac{1}{\cos \delta}.$$

Images reconstructed in this way are shown in Fig. 5a. The deformation here is opposite to that observed in the case when $\alpha \neq 0$, $\beta \neq 0$ and $\varepsilon = 0$, $\delta = 0$, which is shown in Fig. 3a. It is clear that when $\alpha = \varepsilon$ and $\beta = \delta$ the reconstructed images become faithful (Fig. 3).

2.2. Lensless transform Fourier holography

In spite of the well-known differences of these holographic processes, when compared with the Fresnel holography the Fourier hologram retains its ability to record all perspective contractions too. It is well known that in this manner of recording the holograms the reference wave is a spherical wave emitted from a quasi point source. The source and the transmitting object lie in the same ξ, η plane. The light field deriving from interference of the reference wave with the wave diffracted by the object in the hologram plane x, y is

$$\psi(x, y) = i|C| \exp \left\{ \frac{i\pi}{f_1 \lambda} (|x|^2 + |y|^2) \right\} + i|C| \exp \left\{ \frac{i\pi}{f_1} (|x|^2 + |y|^2) \right\} \times$$

$$\begin{aligned} & \times \iint D \left(\frac{\xi'}{\cos \alpha}, \frac{\eta'}{\cos \beta} \right) \exp \left\{ \frac{i\pi}{f_1 \lambda} \left[\left| \frac{\xi'}{\cos \alpha} \right|^2 + \left| \frac{\eta'}{\cos \beta} \right|^2 \right] \right\} \times \\ & \times \exp \left\{ \frac{2\pi}{\lambda f_1} \left(\frac{\xi' x}{\cos \alpha} + \frac{\eta' y}{\cos \beta} \right) \right\} \frac{d\xi' d\eta'}{\cos \alpha \cos \beta}. \end{aligned} \quad (8)$$

In analogy to the above described Fresnel holography, the amplitude transmittance D of the object is written in coordinates $\xi = \frac{\xi'}{\cos \alpha}$ and $\eta = \frac{\eta'}{\cos \beta}$. The axes of the object

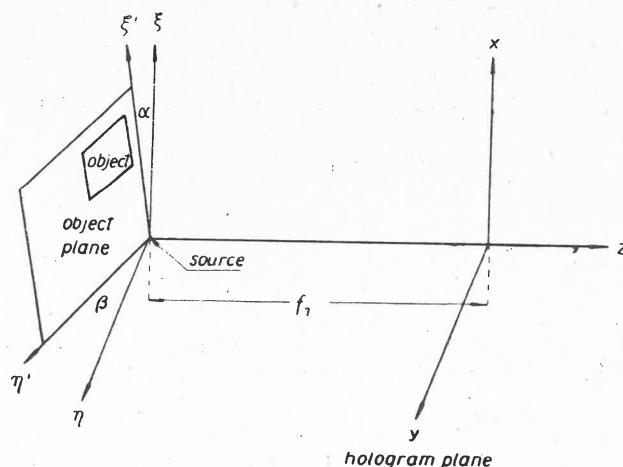


Fig. 6. Coordinate axes used in the description of the construction of lensless Fourier hologram

plane ξ', η' make with the corresponding cartesian coordinate axes ξ, η the angles α and β , what is shown in Fig. 6. Introducing the notation

$$\tilde{D} = D \left(\frac{\xi'}{\cos \alpha}, \frac{\eta'}{\cos \beta} \right) \exp \left\{ \frac{i\pi}{f_1 \lambda} \left(\left| \frac{\xi'}{\cos \alpha} \right|^2 + \left| \frac{\eta'}{\cos \beta} \right|^2 \right) \right\}$$

and applying the Fourier transformation

$$\iint \tilde{D} \left(\frac{\xi'}{\cos \alpha}, \frac{\eta'}{\cos \beta} \right) \exp \left\{ - \frac{2\pi}{f_1 \lambda} \left(\frac{\xi' x}{\cos \alpha} + \frac{\eta' y}{\cos \beta} \right) \right\} \frac{d\xi' d\eta'}{\cos \alpha \cos \beta}$$

we obtain

$$\tilde{\mathcal{D}} \left(\frac{x}{\lambda f_1 \cos \alpha}, \frac{y}{\lambda f_1 \cos \beta} \right). \quad (9)$$

The hologram transmittance can be described as

$$\begin{aligned} T(x, y) = & |C|^2 \cdot \left\{ 1 - \frac{\gamma}{2} \left| \tilde{\mathcal{D}} \left(\frac{x}{\lambda f_1 \cos \alpha}, \frac{y}{\lambda f_1 \cos \beta} \right) \right|^2 - \right. \\ & \left. - \frac{\gamma}{2} \tilde{\mathcal{D}} \left(\frac{x}{\lambda f_1 \cos \alpha}, \frac{y}{\lambda f_1 \cos \beta} \right) - \frac{\gamma}{2} \tilde{\mathcal{D}}^* \left(\frac{x}{\lambda f_1 \cos \alpha}, \frac{y}{\lambda f_1 \cos \beta} \right) \right\}. \end{aligned} \quad (10)$$

The last two terms are responsible for the appearance of twin diffracted waves containing the information about the object.

The real images are obtained by this method in two stages: the hologram is illuminated with a plane wave and then either of the twin beams is focused by a lens. After illuminating the hologram with a plane wave $A \exp\left(-\frac{i2\pi}{\lambda}z\right)$ the light field of one of the twin bundles is

$$\psi(x, y) = \frac{\gamma}{2} \tilde{\mathcal{D}}\left(\frac{x}{\lambda f_2 \cos \alpha}, \frac{y}{\lambda f_2 \cos \beta}\right) A \exp\left(-\frac{i2\pi}{\lambda}d\right)$$

where d is the direction of the diffracted wave. A lens positioned in the way of the beam produces an inverse Fourier transform on it. In the focus plane of the lens, at the distance f_2 , the real image of the object appears. The intensity distribution of this image is:

$$I(\vartheta, \varkappa) = \psi_{\text{im}}(\vartheta, \varkappa) \psi_{\text{im}}^*(\vartheta, \varkappa)$$

where

$$\begin{aligned} \psi_{\text{im}}(\vartheta, \varkappa) = & \frac{\gamma}{2} A |C|^2 \exp\left(-\frac{i2\pi}{\lambda}d\right) \exp\left\{\frac{i\pi}{\lambda f_2}(\vartheta^2 + \varkappa^2)\right\} \times \\ & \times \iint \tilde{\mathcal{D}}\left(\frac{x}{\lambda f_1 \cos \alpha}, \frac{y}{\lambda f_1 \cos \beta}\right) R\left[\frac{x}{\varrho}, \frac{y}{\varrho}\right] \exp\left\{-\frac{i\pi}{\lambda f_2}(\vartheta x + \varkappa y)\right\} dx dy \end{aligned} \quad (11)$$

R determinates here the condition as to the size ϱ of the lens

$$R = \begin{cases} 1 & x \leq \varrho \\ & y \leq \varrho \\ 0 & x \geq \varrho \\ & y \geq \varrho \end{cases}$$

This R is factor governed by the size ϱ of the lens. In practical cases the part of the hologram which is illuminated by a laser beam of finite cross-section is less than the diameter of the lens, so we can put $R = 1$. The integral in equation (11) is the Fourier transform

$$\tilde{D}_{\text{im}}\left(\frac{\vartheta \cos \alpha}{m}, \frac{\varkappa \cos \beta}{m}\right) = \iint \tilde{\mathcal{D}}\left(\frac{x}{\lambda f_1 \cos \alpha}, \frac{y}{\lambda f_1 \cos \beta}\right) \exp\left\{-\frac{i2\pi}{\lambda f_2}(\vartheta x + \varkappa y)\right\} dx dy.$$

Making use of equation (9) we obtain:

$$\tilde{D}_{\text{im}}\left(\frac{\vartheta \cos \alpha}{m}, \frac{\varkappa \cos \beta}{m}\right) = D_i\left(\frac{\vartheta \cos \alpha}{m}, \frac{\varkappa \cos \beta}{m}\right) \exp\left\{\frac{i\pi}{\lambda f_1}\left(\frac{\vartheta^2 \cos^2 \alpha}{m^2} + \frac{\varkappa^2 \cos^2 \beta}{m^2}\right)\right\}. \quad (12)$$

Here, $m = \frac{f_1}{f_2}$.

The resulting distribution of intensity in the focus plane of the lens ϑ, \varkappa is $I(\vartheta, \varkappa)$

$$= |K|^2 D^2 \left(\frac{\vartheta \cos \alpha}{m}, \frac{\varkappa \cos \beta}{m}\right).$$

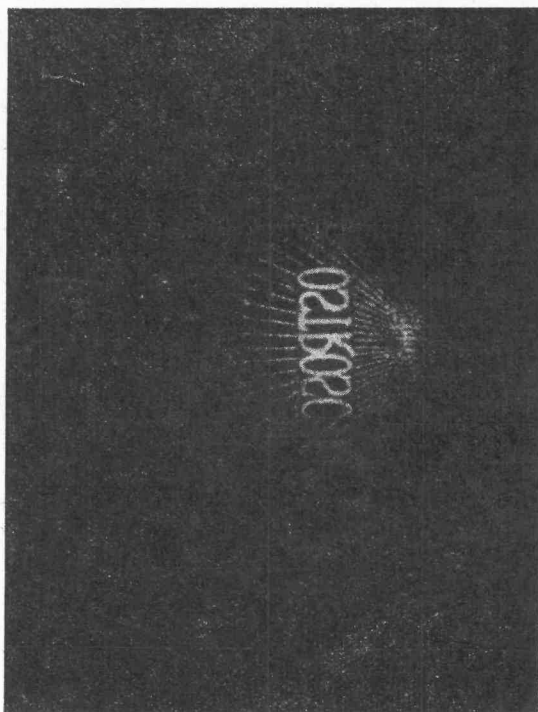


Fig. 7

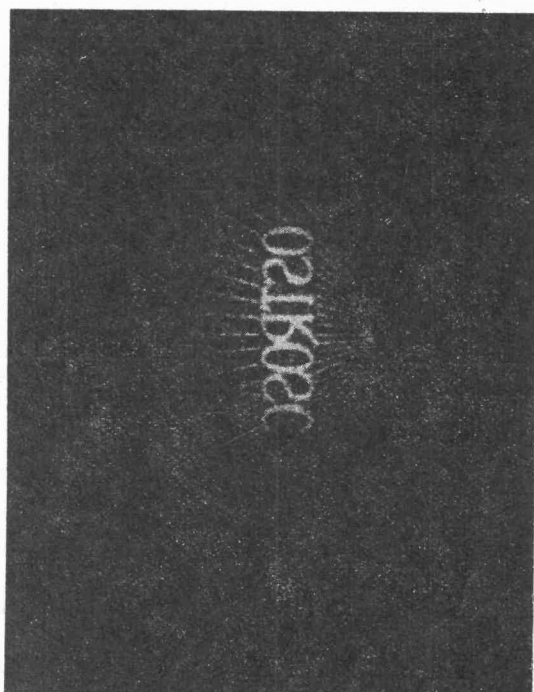


Fig. 7a

Fig. 7. Test image reconstructed from the lensless Fourier hologram (ORWO WP3 Plattes). *a*. The same reconstructed test image when the hologram plane is rotated through an angle of 45° during reconstruction

The observed reconstructed image is magnified by ratio m as a whole and shortened proportionally to $\cos \alpha$ and $\cos \beta$ correspondingly in the direction of the ϑ and ϖ axes.

The deformation can be removed by rotating the hologram during reconstruction. Then the hologram lies in another plane, the coordinates $x'y'$ of which makes with cartesian coordinates x, y angles ε and δ . In this case we change the hologram coordinates so that

$x' = \frac{x}{\cos \varepsilon}$ and $y' = \frac{y}{\cos \delta}$, as shown in Fig. 7. The light field in the image plane changes then in the following way:

$$\begin{aligned} \psi_{\text{im}}(\vartheta, \varpi) &= \frac{\gamma}{2} A |C|^2 \exp(ikd) \exp\left\{\frac{i\pi}{\lambda f_2} (\vartheta^2 + \varpi^2)\right\} \times \\ &\times \iint \tilde{\mathcal{D}}\left(\frac{x}{\lambda f_1 \cos \alpha}, \frac{y}{\lambda f_1 \cos \beta}\right) \exp\left\{-\frac{i\pi}{\lambda f_2} \left(\frac{\vartheta x}{\cos \varepsilon} + \frac{\varpi y}{\cos \delta}\right)\right\} \frac{dx dy}{\cos \varepsilon \cos \delta}. \end{aligned} \quad (13)$$

From this equation after the same treatment we obtain the transformed transmittance

$$\begin{aligned} \tilde{D}_{\text{im}}\left(\frac{\vartheta \cos \alpha}{m \cos \varepsilon}, \frac{\varpi \cos \beta}{m \cos \delta}\right) \\ = D\left(\frac{\vartheta \cos \alpha}{m \cos \varepsilon}, \frac{\varpi \cos \beta}{m \cos \delta}\right) \cdot \exp\left\{\frac{2\pi i}{\lambda f_1} \left(\frac{\vartheta^2 \cos^2 \alpha}{m^2 \cos^2 \varepsilon} + \frac{\varpi^2 \cos^2 \beta}{m^2 \cos^2 \delta}\right)\right\}. \end{aligned} \quad (14)$$

The observed intensity distribution is:

$$I(\vartheta, \varpi) = |K|^2 \left| D^2\left(\frac{\vartheta \cos \alpha}{m \cos \varepsilon}, \frac{\varpi \cos \beta}{m \cos \delta}\right) \right|. \quad (15)$$

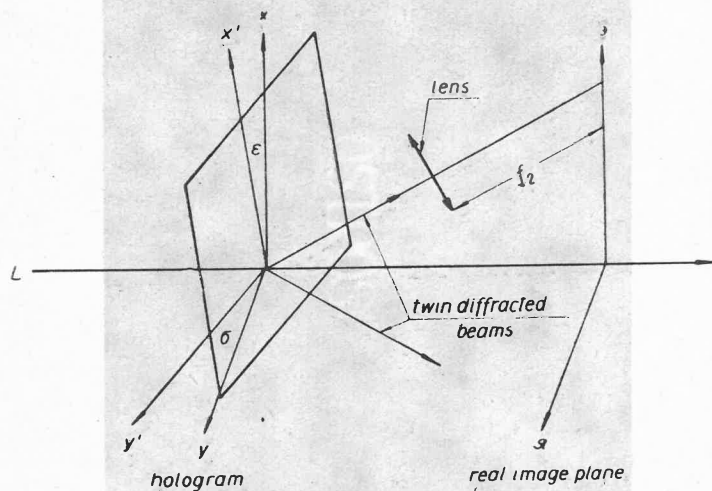


Fig. 8. Coordinate axes used in the description of reconstruction of lensless Fourier hologram

The image is magnified m -times in all; at the same time it is shortened proportionally to $\cos \alpha$ and $\cos \beta$ in the direction of the ϑ and ϖ axes and lengthened proportionally to $\cos \varepsilon$ and $\cos \delta$ in the same directions. In the case when $\alpha = \varepsilon$ and $\beta = \delta$ the reconstructed image

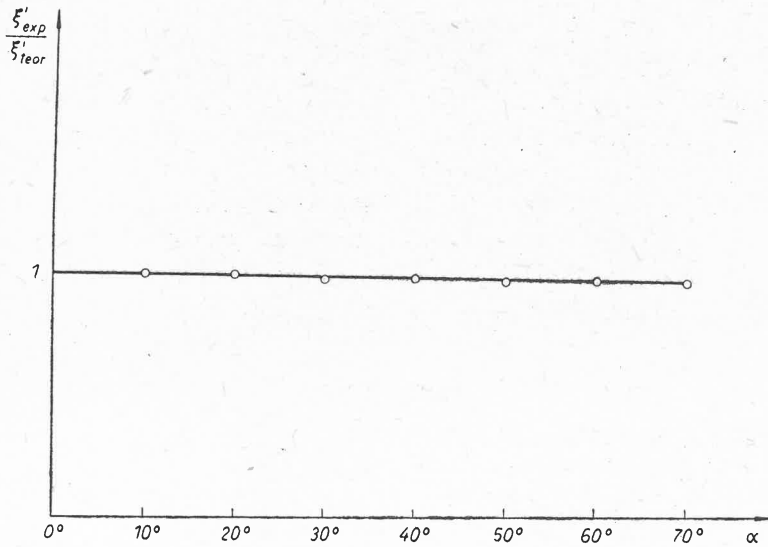


Fig. 9a. Comparison between the experimental data of the shortened side ξ' of the testsquare and the value calculated from the undeformed length ξ by using Eq. (15) for several values of angle α

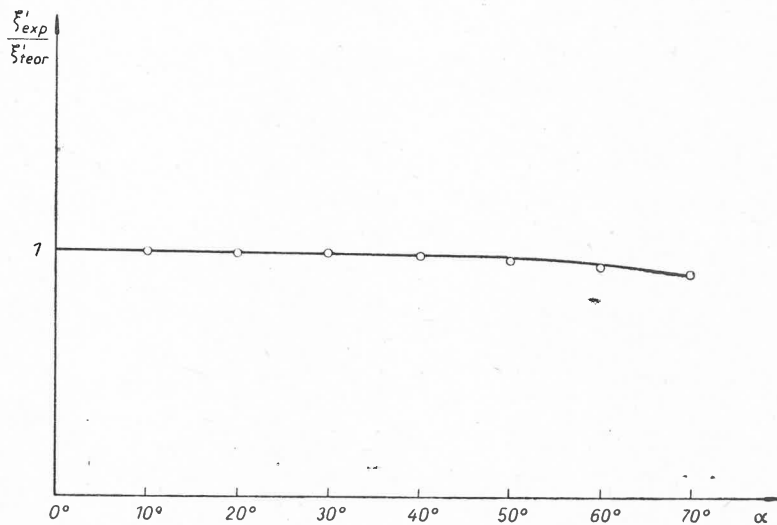


Fig. 9b. Comparison between the experimental data of the lengthened side ξ' of test square and the value calculated from the undeformed length ξ by using Eq. (15) for several values of angle α

becomes faithful with regard to an object seen perpendicularly. For example the reconstructed image of a lensless hologram deformed during reconstruction is shown in Fig. 7a.

The test image in the form of a square with side ξ is recorded by varying the angle α or reconstructed by varying the angle ϵ . The observed deformations of ξ are in good agreement with Eq. (15), as shown in Fig. 9a and 9b.

3. Conclusion

It is clear that on the one hand a hologram is able to record all perspective distortions as all photographic recorders do. Independently of this ability the reconstructed images can be deformed by rotating the hologram during reconstruction. In this way it is possible to create artificially an elongation of the object or remove the perspective shortening which was recorded during construction of the hologram. This behaviour of the hologram is especially reminiscent of lens astigmatism. Treating a hologram like a specific lens we can define the ability to create deformed pictures, depending on the angle which the reconstructing wave makes with the hologram plane, as hologram astigmatism.

REFERENCES

- [1] A. K. Rigler, *J. Opt. Soc. Amer.*, **55**, 1963 (1965).
- [2] A. Kalestyński, B. Smolińska, *Phys. Letters*, **28A**, 590 (1969).
- [3] J. De Velis, G. Reynolds, *Theory and application of holography*, Addison Wesley Publ. Co. Inc. 1967.